Mathematical Problems in Engineering
Volume 5, pp. 97–119
Reprints available directly from the publisher
Photocopying permitted by license only

Multidisciplinary Design Optimization of Film-Cooled Gas Turbine Blades

SHASHISHEKARA S. TALYA[a], J.N. RAJADAS[b] and A. CHATTOPADHYAY[a,*]

[a]*Department of Mechanical and Aerospace Engineering,* [b]*Department of Manufacturing and Aeronautical Engineering Technology, Arizona State University, Tempe, AZ 85287-6106, USA*

(Received 29 July 1998; Revised 21 September 1998; In final form 2 November 1998)

Design optimization of a gas turbine blade geometry for effective film cooling to reduce the blade temperature has been done using a multiobjective optimization formulation. Three optimization formulations have been used. In the first, the average blade temperature is chosen as the objective function to be minimized. An upper bound constraint has been imposed on the maximum blade temperature. In the second, the maximum blade temperature is chosen as the objective function to be minimized with an upper bound constraint on the average blade temperature. In the third formulation, the blade average and maximum temperatures are chosen as objective functions. Shape optimization is performed using geometric parameters associated with film cooling and blade external shape. A quasi-three-dimensional Navier–Stokes solver for turbomachinery flows is used to solve for the flow field external to the blade with appropriate modifications to incorporate the effect of film cooling. The heat transfer analysis for temperature distribution within the blade is performed by solving the heat diffusion equation using the finite element method. The multiobjective Kreisselmeier–Steinhauser function approach has been used in conjunction with an approximate analysis technique for optimization. The results obtained using both formulations are compared with reference geometry. All three formulations yield significant reductions in blade temperature with the multiobjective formulation yielding largest reduction in blade temperature.

Keywords: Multidisciplinary; Optimization; Turbine blade; Film cooling; Heat transfer

* Corresponding author.

INTRODUCTION

In the area of gas turbine technology, the main emphasis has been to increase the efficiency of the turbine. One of the best means of achieving higher efficiency in gas turbine engines is by raising the turbine inlet temperature. But, this brings in the problem of choosing the right materials which can withstand high temperatures and the ease of manufacturing turbine blades using these materials. A method to alleviate this problem, is to design effective turbine blade cooling mechanisms which can keep the turbine blade temperatures below acceptable level. One such method of cooling is by film cooling, wherein a secondary fluid is introduced at discrete locations on the surface of the blade that is exposed to a high temperature environment. This, combined with the flow field around the blade has the advantage of thermal protection not only in the immediate vicinity of injection but, also in the downstream region. An excellent survey of work done on film cooling before 1971 can be found in Goldstein [1]. Langowsky *et al.* [2] did an experimental and numerical investigation of the effect of film cooling on the secondary flow development by simulating cooling air ejection through discrete cells of the computational mesh. Sections of turbine blade requiring intensive cooling are covered over the entire area with holes through which cooling air is ejected. This is called 'full coverage film cooling'. Eckert [3] developed a new method to predict the temperature of this hot section by 'full coverage film cooling' based on two different parameters, θ and K, where, θ is the ratio of the difference in the coolant exit temperature and the free stream temperature to the difference in the wall temperature and free stream temperature. K is the ratio of the difference in the convective heat transfer coefficient when $\theta = 1$ and when $\theta = 0$ to the convective heat transfer coefficient when $\theta = 0$. Heat and mass transfer analogy has been used by Takeishi *et al.* [4] to study film cooling effectiveness on a low-speed stationary cascade and rotating blade. The film cooling effectiveness on the suction surface of the rotating blade agreed well with that on the stationary blade, but a low level effectiveness appeared on pressure surface of rotating blade. Weigand *et al.* [5] used a three-dimensional-Navier–Stokes solver along with an unstructured solution adaptive grid methodology to numerically investigate film cooled turbine rotor. Results showed

significant interaction between the coolant flow and secondary flow near the hub and the tip of the turbine blade. Numerical modeling of a three-dimensional discrete-jet in crossflow problem, typical of a realistic film cooling application in gas turbine was done by Walters *et al.* [6]. They presented results from a series of simulations based on systematic approach to the four critical issues of a computational simulation. These are: (1) proper computational modeling of flow physics; (2) exact geometry and high-quality grid generation; (3) higher order discretization scheme; and (4) effective turbulence modeling. Solutions were obtained with a multiblock, unstructured/adaptive grid, fully explicit, time-marching, Reynolds-averaged Navier–Stokes code with residual smoothing. They found that turbulent anisotropy is still a serious issue to be resolved in the simulation of film cooling problems, especially regarding the lateral spreading of coolant jet. Time resolved measurements of heat transfer on a fully cooled transonic turbine stage was done by Abhari *et al.* [7] who experimentally quantified the influence of three-dimension and unsteady effects on the rotor film cooling process.

The design of turbine blades in gas turbine engines requires the integration of several important disciplines such as aerodynamics, heat transfer and structures. The high temperature environment in the turbine affects the life of the blade and its structural integrity, and efficient removal of heat from the blade interior will help in prolonging blade life. Due to allowable limits on material melting temperature and thermal stresses, the external shape of turbine blade and the position and the size of film cooling holes must be designed such that the maximum and the average temperature in the blade are maintained as low as possible. Since the external flow heats up the blade, effective reduction in temperature can be achieved by appropriately positioning the coolant holes. The size of the coolant hole is also an important criteria to help in reducing the surface temperature of the blade. From a structural point of view, it is important to maintain the blade structure under allowable stress and vibration levels. Thus, effective design of turbine blade involves integration of all the above disciplines.

Formal optimization techniques are being widely used in a variety of engineering design problems today. An extensive amount of work has been done in developing optimization procedures to bring the state

of the art to a very high level [8]. The use of numerical optimization procedures for the design of airfoils has been a subject of considerable interest, primarily for aircraft wing design [9–13]. However, only limited information is available in the applications of formal design optimization procedures for efficient turbine blade design. Chattopadhyay *et al.* [14] developed an optimization procedure for efficient aerodynamic design of turbine blades that successfully eliminated the leading edge velocity spikes without compromising blade performance. Dulikravich *et al.* [15,16] have developed inverse procedures for the design of blade coolant passages with specified temperatures and heat fluxes. Demeulenaere *et al.* [17] developed an iterative procedure for three-dimensional blade design. A transpiration model was used along with a modified Euler solver, in which the target pressure distribution on the blade is imposed to modify the blade shape. A three-dimensional inverse method for the aerodynamic design of turbine blades was developed by Dang *et al.* [18]. The main idea in the method used was to replace the blades with a periodic discrete body-force field. The body-force was included in the equation of motion, and an existing time-marching algorithm was employed to integrate the finite volume formulation of the unsteady Euler equations to a steady-state solution. The blade geometry was modified during the time-marching procedure using the flow-tangency boundary conditions along the blade surface. However, the effect of blade external shape on heat transfer was not considered in these efforts. Also, all the above investigations were based on criteria related to a single discipline. Narayan *et al.* [19] developed a multidisciplinary optimization procedure, integrating aerodynamic and heat transfer effects to design turbine blades. They achieved better aerodynamic design, by reducing velocity spikes associated with blade leading edge on both suction and pressure surface and better heat transfer characteristics by changing the coolant path geometry and the external blade shape.

In the present work, a multiobjective shape optimization procedure is presented for the design of turbine blades. The effect of film cooling of the surface of the turbine blade has been considered. Film coolant holes are modeled by specifying the boundary nodes corresponding to the position of each hole. The initial position of the film cooling holes is decided based on the temperature distribution within the blade with no film cooling. Once the position of the film cooling holes are

established, the blade surface boundary condition is changed accordingly to take into consideration the changes caused in the flow field due to the blowing of coolant air through these holes. An appropriate model is developed for the blade section and the film cooling holes which are included during design by incorporating them as design variables, and imposing the necessary constraints on them to get a feasible design. For film cooling holes, constraints are imposed on the size and position of each hole. This is done to prevent the coolant holes from getting very close to one another during the optimization cycle and also to avoid the possibility of ending up with large coolant holes that are not practically feasible.

BLADE MODEL

In the present work, only a two-dimensional model has been considered. Therefore, only the blade cross-sectional shape is modeled. The airfoil external shape and film cooling holes are modeled as shown in Fig. 1. The suction surface and the pressure surface are represented by a series of cubic splines of the form,

$$y = c_0 + c_1 x + c_2 x^2 + c_3 x^3, \tag{1}$$

where x is the meridional coordinate, y is the tangential coordinate and c_0, c_1, c_2 and c_3 are the spline coefficients. The trailing edge is also represented by cubic splines of the form shown above. The leading edge geometry is represented by cubic splines, but with the equation,

$$x = c_0 + c_1 y + c_2 y^2 + c_3 y^3. \tag{2}$$

This helps maintain a smooth geometry at the leading edge. Continuity of function and slope are imposed at the end points of the splines. The tangential (y) coordinate and the slope of the surface at the spline joints on each surface are used as design variables in the optimization. The position of the film cooling holes are indicated by specifying the respective nodes on the blade surface. Further details on the modeling of coolant holes are provided in the analysis section of this paper. The position, size, blowing rate, temperature and angle of

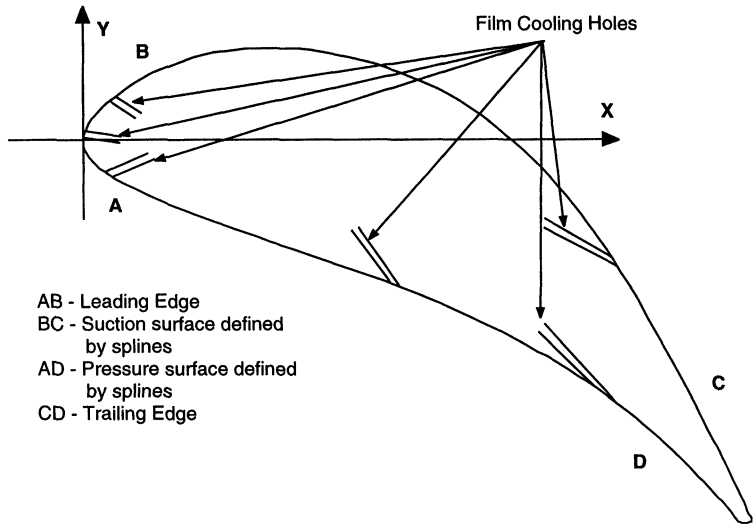

FIGURE 1 Blade model.

blowing of film cooling holes are used as design variables in the optimization procedure. The trailing edge shape is held fixed in order to satisfy the design requirement that the throat length of the turbine blade cascade remain fixed.

ANALYSIS

Aerodynamic and Heat Transfer Analysis

A rapid quasi-three-dimensional computational fluid dynamics (CFD) code (RVCQ3D) [20] is used to solve for the flow fields outside the blade. A body-fitted grid for this purpose is generated using the GRAPE code (GRids about Airfoils using Poisson's Equation) developed by Sorenson [21,22]. The code allows the arbitrary specification of inner and outer boundary points and then generates interior points as a solution to Poisson equation. Forcing terms in the Poisson equation are chosen such that the desired grid spacing and intersection angles may be maintained at the inner and outer boundary. C-grid topology is used to grid the flow region. The CFD code solves the

unsteady Euler or thin-layer Navier–Stokes equations in a body-fitted coordinate system. It accounts for the effects of rotation, radius change, and stream surface thickness. The Bladwin–Lomax eddy viscosity model is used for turbulent flows. The equations are solved using a two-stage Runge Kutta scheme made efficient by the use of vectorization, a variable time step, and a flux based multigrid scheme. The governing equations are written in a (m, θ) coordinate system, where, m indicates the flow direction and θ is perpendicular to the flow and are then transformed to a general body-fitted (ξ, η) system using standard methods. The thin-layer approximation is used to eliminate all viscous derivatives in the streamwise ξ direction. The final equations are:

$$\frac{\partial \mathbf{q}}{\partial t} + \frac{\partial \mathbf{F}}{\partial \xi} + \frac{\partial}{\partial \eta}(\mathbf{G} - Re^{-1}\mathbf{S}) = \mathbf{K}, \tag{3}$$

where $\mathbf{q}$, $\mathbf{F}$, $\mathbf{K}$, $\mathbf{G}$ are the inviscid flux terms and $\mathbf{S}$ is the viscous flux term.

A one-dimensional flow equation with area change is solved analytically to produce initial conditions that smoothly connect the specified inlet and exit values. At the inlet, total pressure, total temperature and whirl are specified. Density and energy are found using isentropic relations. At the exit the static pressure is specified and the other flow quantities are found using first order extrapolation. For the blade surface, temperature is specified (adiabatic in this case) and pressure is calculated from the normal momentum equation. For the film cooling, the blowing rate, temperature and pressure were specified as multiples of the freestream mass flow rate, freestream temperature and freestream pressure respectively at the positions where film cooling holes are located. Each of these multiplying factors is then used as a design variable in the optimization procedure. The flow angle at hole points was fixed at the geometric angle of the hole themselves, which is at 30° to the blade in the spanwise direction. The flow angle at which the coolant air is discharged, is also taken as a design variable. The governing equations are solved with the appropriate boundary and initial conditions to give the velocity and temperature field in the flow region around the turbine blade. To evaluate for the temperature distribution inside the airfoil the

two-dimensional conduction problem, governed by the following equation:

$$\frac{\partial}{\partial x}\left(\kappa\frac{\partial T}{\partial x}\right)+\frac{\partial}{\partial y}\left(\kappa\frac{\partial T}{\partial y}\right)=0, \tag{4}$$

where, T is the local blade temperature and κ is the thermal conductivity of the blade material has been solved. The boundary value problem is numerically solved using the finite element method [23]. The computational domain is discretized using linear triangular elements. Figure 2 shows a typical computational mesh used in the finite element analysis. Since the geometry of the blade changes during optimization, after each cycle remeshing is done on the computational domain. The boundary conditions are then specified at each node on the boundary. Three types of boundary conditions can be used in the solution. They are the Dirichlet condition, the Neumann condition and the convective boundary condition. In the present problem, Dirichlet type boundary condition is specified. Using the Galerkin

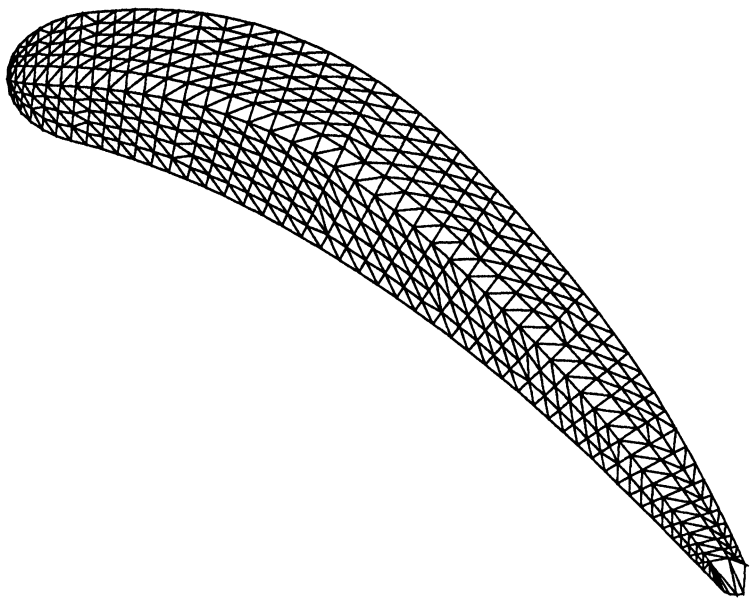

FIGURE 2 Finite element mesh.

approach, the above boundary value problem (Eq. (4)) is reduced to the following system of linear simultaneous equations for the unknown nodal temperatures:

$$[\mathbf{K}]\bar{\mathbf{T}} = \bar{\mathbf{F}}. \tag{5}$$

Here, $[\mathbf{K}]$ is the global stiffness matrix and $\bar{\mathbf{F}}$ is the forcing vector. These are evaluated using the finite element formulation and the boundary conditions. The solution of Eq. (5) yields the nodal temperatures, $\bar{\mathbf{T}}$.

Optimization Formulation

In the design of complex engineering systems, it is often difficult to select a single objective function which will satisfy all of the desired design requirements. Several techniques have previously been developed for multiobjective optimization. Most of the previous efforts to include multiple objective functions in a numerical optimization method can be separated into two techniques. The first is to form a single composite objective function as some combination of the original objective functions such as the summation of each objective function multiplied by a judgmental weighting factor. An example of this approach is the utility function method. The second approach is to solve the optimization problem once for each single objective function and then to use the resulting optimum objective function or design variable vector as a target, solving an additional optimization problem to attain a suitable compromise. Examples of this approach are the global criterion formulation, game theory approach, goal programming method, and goal attainment method.

In general, an optimization problem at each level involves multiple objective functions and constraints. Since traditional optimization techniques address problems with a single objective function, it is essential to use formal multiobjective formulation techniques for such applications. For this purpose the Kreisselmeier–Steinhauser (K–S) function [24] approach is used in which multiple objective functions and constraints are combined using the K–S function to form a single composite function. This composite function is then used to solve the optimization problem. To solve the unconstrained nonlinear optimization problem, the Broyden–Fletcher–Goldfarb–Shanno (BFGS)

algorithm [25] has been used in the present work. The following section briefly describes the K–S method.

The K–S Function Method

The K–S function approach [24] has been used in various design problems. In this approach, the original objective functions and/or constraints are scaled into reduced objective functions. Depending on whether the individual objective functions are to be minimized or maximized, these reduced objective functions assume one of the two following forms:

$$F_k^*(\Phi) = \frac{F_k(\Phi)}{F_{k_o}} - 1.0 - g_{\max} \leq 0, \quad k = 1, \ldots, \text{NOBJ}_{\min}, \tag{6a}$$

$$F_k^*(\Phi) = 1.0 - \frac{F_k(\Phi)}{F_{k_o}} - g_{\max} \leq 0, \quad k = 1, \ldots, \text{NOBJ}_{\max}, \tag{6b}$$

where F_{k_o} represents the original value of the kth objective function (F_k) calculated at the beginning of each cycle and Φ is the design variable vector. $g_{\max}$ represents the largest constraint in the original constraint vector, $g_j(\Phi)$, and is held constant during each cycle. The reduced objective functions are analogous to constraints. Therefore, a new constraint vector, $f_m(\Phi)$ ($m = 1, 2, \ldots, M$ where $M = \text{NC} + \text{NOBJ}$), that includes the original constraints and the reduced objective functions (Eqs. (6a) or (6b)), is introduced. The new objective function to be minimized is defined using the K–S function as follows:

$$\mathbf{F}_{\text{KS}}(\Phi) = f_{\max} + \frac{1}{\rho} \log_e \sum_{m=1}^{M} e^{\rho(f_m(\Phi) - f_{\max})}, \tag{7}$$

where $f_{\max}$ is the largest constraint in the new constraint vector $f_m(\Phi)$ and, in general, is not equal to $g_{\max}$. The composite function $F_{\text{KS}}(\Phi)$, which represents an envelope function of the original objective functions and constraints, can now be minimized using a suitable unconstrained optimization technique.

An example of how the K–S function formulation works is illustrated in Fig. 3(a) and (b) for an optimization problem with two objective functions to be minimized and one constraint. The objective

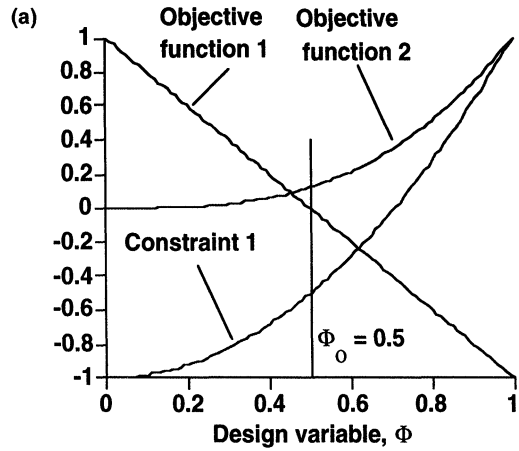

FIGURE 3(a) Original objective functions and constraints.

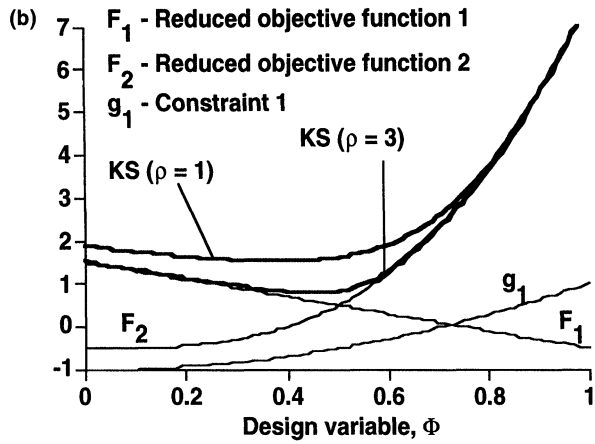

FIGURE 3(b) K–S function envelope.

functions and the constraint are functions of single design variable, ϕ. An initial design point of $\phi_o = 0.5$ is used in the example. At this point, the constraint is satisfied and, therefore, g_{max} is negative. The original constraint and the two additional constraints from the two reduced objective functions, calculated from Eq. (6a), are shown in Fig. 3(b) along with the K–S function envelopes for two different values of ρ. Since g_{max} is negative, the constraints due to the two reduced objective

functions are positive and hence, violated, at the initial design point, ϕ_o. It is seen in Fig. 3(b) that for $\rho = 1$, the K–S function includes contributions from all the three constraints. For a larger value of $\rho = 3$, the K–S function gets a stronger contribution from the largest constraint and weaker contributions from the other two. Thus large values of ρ "draw down" the K–S function closer to the value of the largest constraint. The value of ρ may change from cycle to cycle. It is progressively increased so that, as the optimization proceeds, the K–S function more closely represents only the largest constraint (or the most violated reduced objective function).

Approximate Analysis

The optimization techniques used here are gradient-based and hence require evaluations of the objective functions and constraints many times during every iteration of optimization. Since it is computationally expensive to evaluate these functions through exact analysis at all times, an approximate analysis technique is used within each iteration of the optimization. The two-point exponential approximation technique developed by Fadel *et al.* [26], has been found to be well suited for nonlinear optimization problems and has been used in the present problem for approximating the objective functions and the constraints within the optimizer. This technique takes its name from the fact that the exponent used in the expansion is based upon gradient information from the previous and current design cycles. The technique is formulated as follows.

$$\hat{\mathbf{F}}(\Phi) = \mathbf{F}(\Phi_1) + \sum_{n=1}^{\mathrm{NDV}} \left[\left(\frac{\phi_n}{\phi_{1_n}} \right)^{p_n} - 1.0 \right] \frac{\phi_{1_n}}{p_n} \frac{\partial \mathbf{F}}{\partial \phi_n}(\Phi_1), \tag{8}$$

where $\hat{F}_k(\Phi)$ is the approximation to the objective function F_k at a neighboring design point Φ, based on its values and its gradients at the current design point Φ_1 and the previous design point Φ_0. The approximate values for the constraints, $\hat{g}_j(\Phi)$, are calculated in a similar fashion. The exponent p_n, in Eq. (8) is defined as:

$$p_n = \frac{\log_e\{\partial \mathbf{F}(\Phi_0)/\partial \phi_n\} - \log_e\{\partial \mathbf{F}(\Phi_1)/\partial \phi_n\}}{\log_e\{\phi_{0_n}\} - \log_e\{\phi_{1_n}\}} + 1.0. \tag{9}$$

The exponent p_n can be considered as a "goodness of fit" parameter, which explicitly determines the trade-offs between traditional and reciprocal Taylor series based expansions (also known as a hybrid approximation technique). It can be seen from Eq. (8) that, in the limiting case when $p_n = 1$, the expansion is identical to the first order Taylor series and when $p_n = -1$, the two-point exponential approximation reduces to the reciprocal expansion form. In the present work, the exponent is defined to lie within this interval, $-1 \leq p_n \leq 1$. If the exponent p_n is greater than 1, it is set equal to 1 and if p_n is less than -1, it is set equal to -1. Equations (8) and (9) indicate that many singularity points may exist in the use of this method and, hence, care must be taken to avoid such points. In the present study, when singularity problems arise, the approximation technique is reduced to the linear Taylor series expansion ($p_n = 1$).

RESULTS

The procedure described above is used to optimize an existing turbine blade geometry [20] for effective film cooling. The major design objective is to minimize the blade interior temperature by a combination of shape optimization and film cooling. The parameters associated with both the blade shape and film cooling (such as size of hole, blowing rate etc.) form the set of design variables. The reference blade geometry (airfoil) is defined by a set of geometric parameters (design variables) presented in Tables I and II. Film cooling is characterized by the position of the coolant holes, the blowing rate, Θ (ratio of temperature of film cooling air to the freestream temperature) and angle of blowing, as indicated in Table III. Four cubic splines have been used to describe the suction and pressure surfaces of the blade and the coordinates and the slopes at the spline end points for each spline are given in Tables I and II. Six coolant holes are used to film cool the surface of the blade. Their position and the associated parameters are given in Tables III. The flow field outside the blade is discretized using the GRAPE code [21,22] which generates a two-dimensional grid that covers the entire flow field with 151 points in the x-direction and 81 points in the y-direction. The surface of the airfoil is represented by 110 nodes. This number is doubled for use in the

TABLE I Spline design variables (suction surface)

Design variables	*Reference*	*Single objective function (min. average blade temperature)*	*Single objective function (min. maximum blade temperature)*	*Two objective function (min. ave. and max. blade temperature)*
Spline Joint 1:				
y-Coord. at spline joint	8.089E−02	−8.171E−02	8.848E−01	7.932E−02
Slope at spline joint	1.3162	1.3367	1.3154	1.313
Spline Joint 2:				
y-Coord. at spline joint	1.2547E−01	1.3335E−01	1.3329E−01	1.2382E−01
Slope at spline joint	2.2429E−01	2.198E−01	2.3803E−01	2.2233E−01
Spline Joint 3:				
y-Coord. at spline joint	−1.844E−01	−1.879E−01	−1.735E−01	−1.856E−01
Slope at spline joint	−1.5963	−1.586	−1.6073	−1.6003
Spline Joint 4:				
y-Coord. at spline joint	−7.892E−01	−7.927E−01	−7.276E−01	−8.049E−01
Slope at spline joint	−2.865	−2.7263	−2.6984	−1.2782
Spline Joint 5:				
y-Coord. at spline joint	−9.181E−01	−9.525E−01	−9.211E−01	−9.181E−01
Slope at spline joint	−3.239	−3.1444	−3.0434	−3.2074

TABLE II Spline design variables (pressure surface)

Design variables	*Reference*	*Single objective function (min. ave. blade temperature)*	*Single objective function (min. max. blade temperature)*	*Two objective function (min. ave. and max. blade temperature)*
Spline joint 1:				
y-Coord. at spline joint	−8.529E−02	−8.496E−02	−7.839E−02	−8.689E−02
Slope at spline joint	−1.2781	−1.2571	−1.277	−1.28152
Spline joint 2:				
y-Coord. at spline joint	−1.345E−01	−1.316E−01	−1.264E−01	−1.361E−01
Slope at spline joint	−4.849E−01	−4.94E−01	−4.562E−01	−4.852E−01
Spline joint 3:				
y-Coord. at spline joint	−5.076E−01	−5.162E−01	−4.775E−01	−5.078E−01
Slope at spline joint	−1.133	−1.1158	−1.1258	−1.1372
Spline joint 4:				
y-Coord. at spline joint	−9.639E−01	−9.506E−01	−9.476E−01	−9.684E−01
Slope at spline joint	−1.5103	−1.5129	−1.5179	−1.1513
Spline joint 5:				
y-Coord. at spline joint	−1.005	−1.0265	−1.01867	−1.03978
Slope at spline joint	−7.856E−01	−7.778E−01	−8.087E−01	−0.78694

TABLE III Film cooling design variables

Design variables	*Reference*	*Single objective function (min. average blade temperature)*	*Single objective function (min. maximum blade temperature)*	*Two objective function (min. ave. and max. blade temperature)*
P1	(0.8922, −0.902) (0.8656, −0.862)	(0.8794, −0.861) (0.8510, −0.819)	(0.9418, −0.897) (0.8793, −0.861)	(0.8794, −0.864) (0.8510, −0.822)
P2	(0.4977, −0.405) (0.4468, −0.357)	(0.4724, −0.361) (0.4211, −0.317)	(0.5228, −0.408) (0.4724, −0.361)	(0.5228, −0.409) (0.4724, −0.362)
P3	(0.1257, −0.139) (0.0857, −0.124)	(0.1067, −0.124) (0.0655, −0.111)	(0.1487, −0.141) (0.0858, −0.118)	(0.1487, −0.143) (0.1067, −0.126)
P4	(0.04286, 0.097) (0.0805, 0.122)	(0.0607, 0.1135) (0.1019, 0.1276)	(0.0429, 0.1003) (0.0805, 0.1221)	(0.0279, 0.0811) (0.0607, 0.1137)
P5	(0.6843, −0.262) (0.7312, −0.342)	(0.6843, −0.240) (0.708, −0.282)	(0.7312, −0.324) (0.7756, −0.409)	(0.7080, −0.286) (0.7312, −0.327)
P6	(0.9241, −0.758) (0.9457, −0.819)	(0.924, −0.758) (0.9354, −0.789)	(0.9458, −0.819) (0.9639, −0.873)	(0.9354, −0.789) (0.9458, −0.819)
Blowing rate	0.7	0.612	0.617	0.588
Θ	0.7	0.652	0.643	0.621
Angle of blowing of film cooling air	30.0	26.21	24.58	24.35

Pi, $i = 1, \ldots, 6$: position of film cooling hole i.

mesh generation code for finite element analysis of the interior of the blade. The blade interior is discretized using approximately 1700 nodes resulting in approximately 3100 elements. Since an adaptive mesh generation procedure is used to generate the finite element mesh, the discretization of the computational domain inside the blade changes after each cycle of optimization. For the external flow, the following flow properties are used: Prantl number (Pr) = 0.72 (air), Reynold's number (Re) = 6.07×10^6 (based on reference conditions), Mach number (Ma) = 0.21, thermal conductivity (κ) = 0.06115 W/m °C, kinematic viscosity = 9.1×10^{-5} m^2/s. For the blade, the thermal conductivity (κ) = 34.62 W/m °C.

Three problems have been considered in this paper. The first problem is that of minimizing the blade average temperature with an upper bound constraint on the maximum blade temperature. The second problem involved minimizing maximum blade temperature with an upper bound constraint on the average blade temperature. In the third problem, both the average and the maximum blade

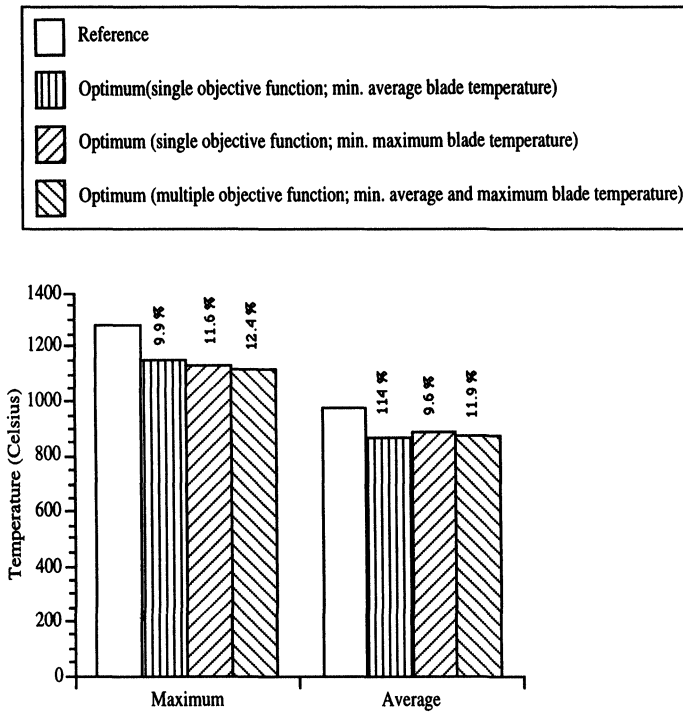

FIGURE 4 Comparison of blade temperatures.

temperatures were minimized. Figure 4 shows the comparison between the reference and optimum values of the maximum and average temperatures in the blade section for the three problems. For the reference configuration, the maximum temperature (T_{max}) is 1278.09°C and the average temperature (T_{ave}) is 978.2°C. In all the three formulations, there is a significant reduction in temperatures. For the single objective function formulation (min. average blade temperature), the average temperature has been reduced by 11.4% and the maximum temperature has been reduced by 9.9%. When the objective function is changed to minimizing the maximum average temperature (with a corresponding constraint on the maximum temperature), the maximum blade temperature is reduced by 11.6% which is a much higher reduction compared to the previous formulation. The average blade temperature for this formulation has been

reduced by 9.6%. For the case of multiple objective function (minimize average and maximum blade temperatures) both the maximum and average temperatures have been reduced (11.9% and 12.4%, respectively) to a larger extent than the above two cases. These reductions in temperature are due to changes in the blade external shape and changes in the film cooling parameters (position, blowing rate, temperature and angle of blowing) associated with the film cooling holes.

Figures 5–7 compare the reference geometry and the optimum geometries obtained from the three formulations. In all three formulations, one can observe that the blade shape and film cooling parameters have changed but not by the same extent. However, there are some features that are common to all three cases. The extent of the shift in the coolant hole position is towards the hot spots on the blade surface as seen in the temperature distribution in the reference blade (Fig. 8). The shift for the multiobjective formulation is less than the other two cases. This might be because of a balancing effect between minimizing the two objective functions as compared to minimizing a

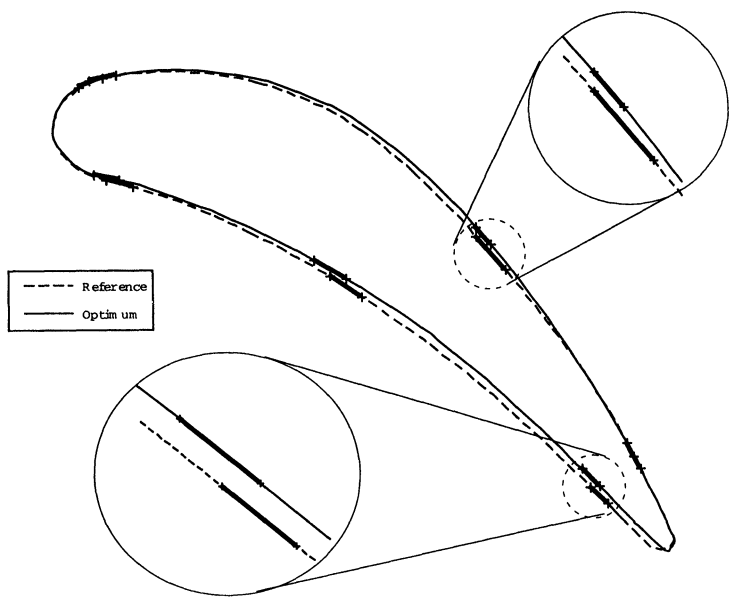

FIGURE 5 Comparison of airfoil geometry; single objective function (min. average blade temperature).

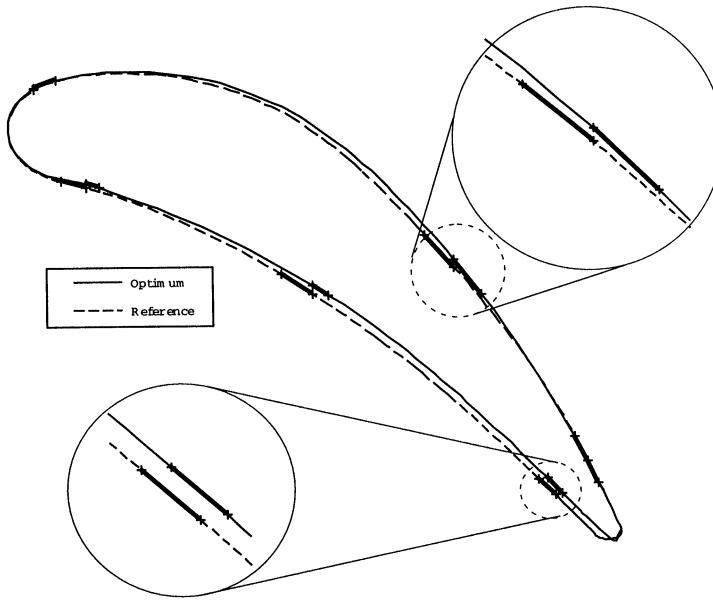

FIGURE 6 Comparison of airfoil geometry; single objective function (min. maximum blade temperature).

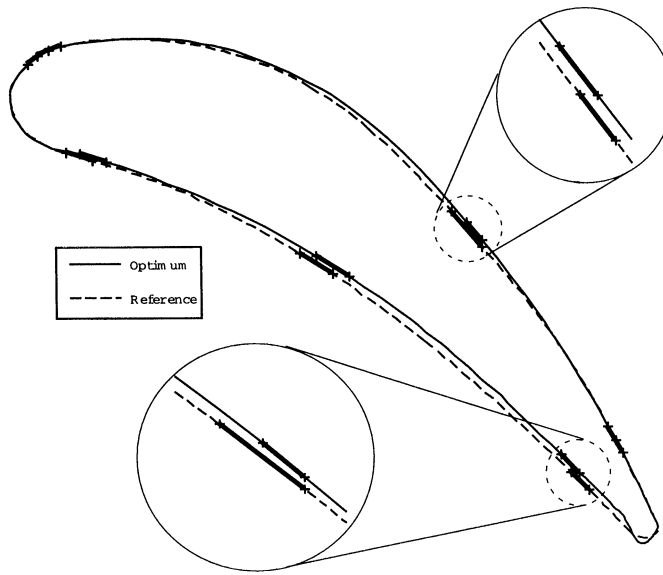

FIGURE 7 Comparison of airfoil geometry; multiple objective function (min. average and maximum blade temperature).

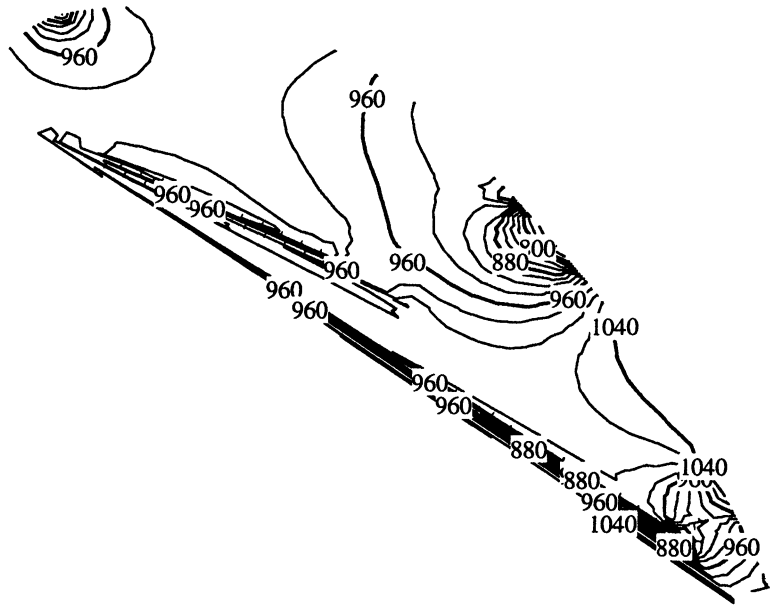

FIGURE 8 Temperature distribution for reference blade.

single objective function. As seen in Table III, the value of the blowing rate, temperature and angle of blowing of film cooling air has decreased for all three cases. A lower film cooling air temperature results in greater reduction in the temperature of the main flow. The decrease in the angle of blowing directs the film cooling air along the blade surface thus protecting the blade surface from the high temperature main flow. For the multiobjective case, the decrease is more when compared to the single objective case. Since the multiobjective formulation needs to minimize two objective functions the reduction has to be more to achieve reasonable reduction in temperatures. The temperature distributions for the three cases considered are presented in Figs. 9–11 respectively. The favorable redistribution of temperature in the optimum configurations can be seen from these figures.

The single objective formulation in which the average blade temperature is minimized converges in 15 cycles and the formulation in which the maximum blade temperature is minimized converges in 14 cycles. The multiple objective formulation, in which both the maximum and average blade temperatures are minimized converges in

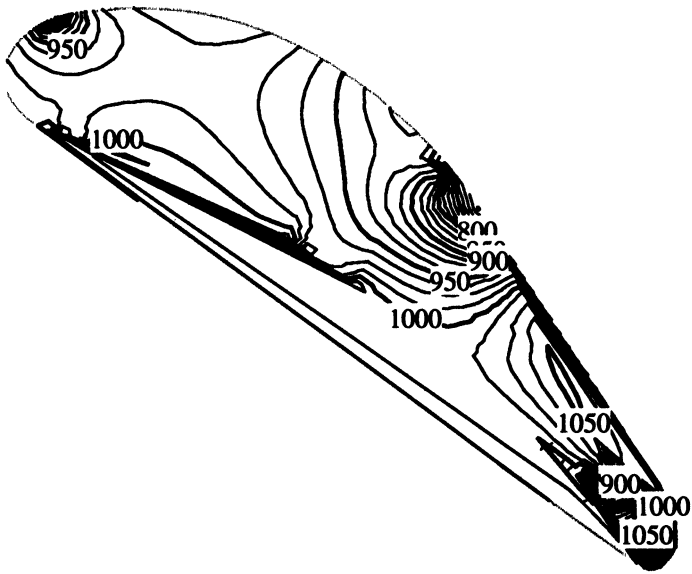

FIGURE 9 Temperature distribution for optimum blade; single objective function (min. average blade temperature).

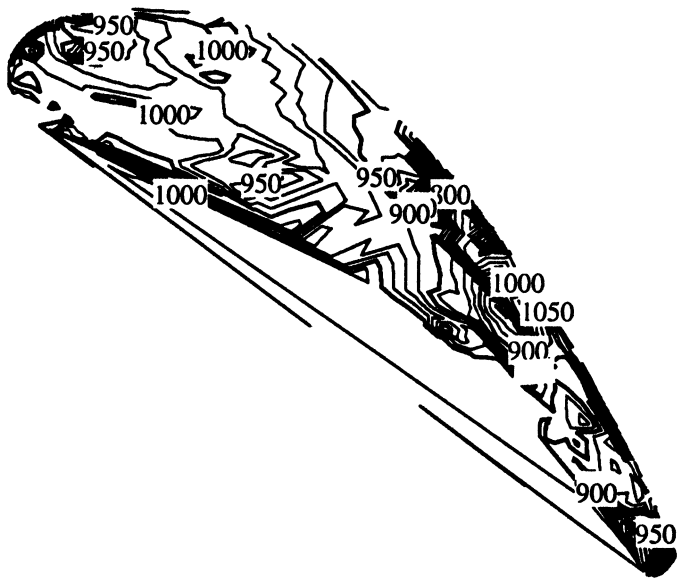

FIGURE 10 Temperature distribution for optimum blade; single objective function (min. maximum blade temperature).

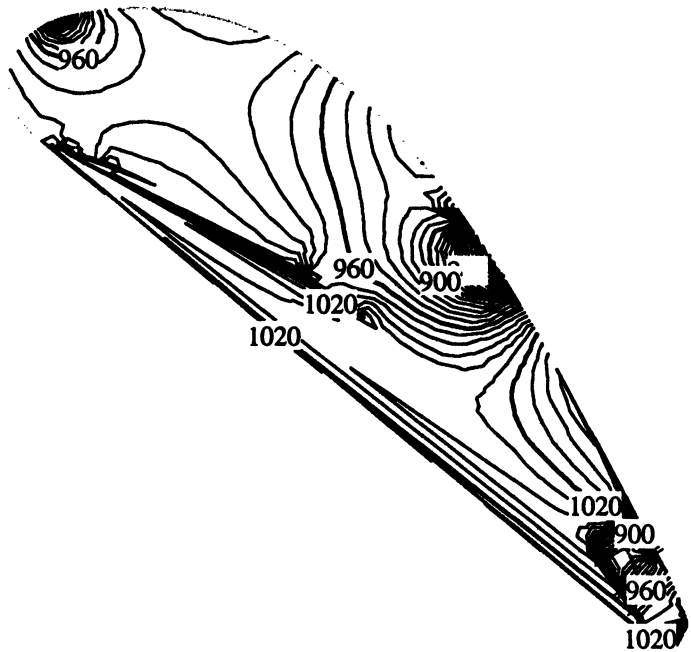

FIGURE 11 Temperature distribution for optimum blade; multiple objective function (min. average and maximum blade temperature).

15 iterations. This means that the computational effort required by all the three formulations is almost the same. But, greater reduction in blade temperature is achieved in multiobjective formulation. This clearly indicates that the multiobjective formulation is better suited for such a multifaceted optimization problem.

CONCLUDING REMARKS

A multiobjective optimization procedure with the integration of aerodynamics and heat transfer has been developed for the design of gas turbine blades to achieve efficient film cooling. Three different formulations are used to study the design problem. In the first one, the average blade temperature is chosen as the objective function to be minimized. In the second one, the maximum blade temperature is chosen as the objective function to be minimized. In the third

formulation, the blade average and maximum temperatures are chosen as objective functions. The CFD code, RVCQ3D, is used to solve for the flow field outside the blade and the finite element method is used for the heat transfer analysis in the blade interior. Film cooling is incorporated by appropriately changing the boundary conditions on the surface of the blade at the nodes where film cooling holes exist. The following observations are made from this study:

(1) All three optimization formulations are very effective in modifying the blade external and film cooling parameters and yield significant reductions in maximum and average temperatures of the blade.
(2) The reductions in the blade temperatures are due to the redistribution of temperature in the blade section, caused by the shifting of coolant hole position and corresponding reduction in blowing rate, temperature of coolant air and decrease in angle of blowing.
(3) The multiobjective formulation yields larger reduction in average and maximum blade temperature when compared to the single objective formulation.
(4) The multiobjective formulation predicts reduced blowing rate, reduced temperature and reduced angle of blowing of film cooling air when compared to the single objective formulation.

Acknowledgments

This research was supported by Allied Signal Aerospace Company, Contract No. NAS 3-27752, Technical Monitor, Dr. Yong Kim.

References

[1] J. Goldstein, Film cooling, *Advances in Heat Transfer*, Academic Press, New York and London, 1971, Vol. 7, pp. 321–379.
[2] Langowsky and D.T. Vogel, The influence of film cooling on the secondary flow in a turbine stator – An experimental and numerical investigation, *31st AIAA/ASME/SAE/ASEE Joint Propulsion Conference and Exhibit*, July 10–12, 1995, San Diego California.
[3] R.G. Eckert, Analysis of film cooling and full-coverage film cooling of gas turbine blades, ASME Paper No. 95-GTJ-2.
[4] S. Takeshi, T. Aoki, Sato and K. Tsukagoshi, Film cooling on a gas turbine rotor blade, ASME Paper No. 91-GT-279.
[5] Weigand and S.P. Harasgama, Computations of a film cooled turbine rotor blade with non-uniform inlet temperature distribution using a three-dimensional viscous procedure, ASME Paper No. 94-GT-15.

[6] K. Walters and J.H. Leylek, A systematic computational methodology applied to a three-dimensional film-cooling flowfield, *Journal of Turbomachinery*, **119**, 1997, 777–785.
[7] S. Abhari and A.H. Epstein, An experimental study of film cooling in a rotating transonic turbine, ASME Paper No. 92-GT-201.
[8] Ashley, On making things the best – Aeronautical use of optimization, *AIAA Journal of Aircraft*, **19**(1), 1982.
[9] S. Hague, H.L. Rozendaal and F.A. Woodward, Application of multivariable search techniques to optimal aerodynamic shaping problems, *Journal of Aerospace Sciences*, **15**(6), 1968, 283–296.
[10] N. Vanderplaats, R.M. Hicks and E.M. Murman, Application of numerical optimization techniques to airfoil design, *Proc. Aerodynamic Analyses Requiring Advanced Computers*, Part II, Langley Research Center, Hampton, Virginia, 1975.
[11] N. Vanderplaats and R.M. Hicks, Numerical airfoil optimization using a reduced number of design coordinates, NASA TMX-73, 151, 1976.
[12] Jameson, Aerodynamic design via control theory, *Journal of Scientific Computing*, **3**, 1988, 233–260.
[13] J-Chung Chang and F.J. Torres, Wind design code using three dimensional euler equations and optimization, *AIAA Aircraft Design Systems and Operations Meeting*, Baltimore, Maryland, 1991.
[14] Chattopadhyay, N. Pagaldipti and K.T. Chang, A design optimization procedure for efficient turbine airfoil design, *Journal of Computers and Mathematics with Applications*, **26**(4), 1993, 21–31.
[15] S. Dulikravich and T.J. Martin, Three-dimensional coolant passage design for specified temperature and heat fluxes, AIAA Paper No.94-0348, *32nd Aerospace Sciences Meeting and Exhibit*, Reno, Nevada, 1994.
[16] S. Dulikravich and T.J. Martin, Inverse design of super elliptic coolant passages in coated turbine blades with specified temperatures and heat fluxes, AIAA Paper No. 92-4714, *4th AIAA/USAF/NASA/OAI Symposium on Multidisciplinary Analysis and Optimization*, Cleveland, Ohio, 1992.
[17] Demeulenaere and R. Van den Braembussche, Three-dimensional inverse method for turbomachinery blade design, *Journal of turbomachinery*, **120**, 1998, 247–255.
[18] Dang and V. Isgro, Euler-based inverse method for turbomachinery blades Part 1: Two-dimensional cascade, *AIAA Journal*, **33**(12), 1995, 2309–2315.
[19] R. Narayan, A. Chattopadhyay, N. Pagaldipti and S. Zhang, Integrated aerodynamics and heat transfer optimization procedure for turbine blade design, AIAA-95-1479-CP.
[20] V. Chima, Explicit multigrid algorithm for quasi-three-dimensional viscous flows in turbomachinery, *Journal of Propulsion*, **3**(5), 1987, 397–405.
[21] L. Sorenson, A computer program to generate two-dimensional grids about airfoils and other shapes by the use of poisson's equation, NASA TM-81198, 1980.
[22] L. Steger and R.L. Sorenson, Automatic mesh point clustering near a boundary in grid generation with elliptic partial differential equations, *Journal of Computational Physics*, **33**(3), 1979, 405–410.
[23] J. Segerlind, *Applied Finite Element Analysis*, second edn. John Wiley and Sons, 1984.
[24] A. Wrenn, An indirect method for numerical optimization using the Kreisselmeier–Steinhauser function, NASA Contract report No. 4220.
[25] T. Haftka, Z. Gurdal and M.P. Kamat, Elements of structural optimization, second revised edn. Kluwer Academic Publishers, Dordrecht, The Netherlands.
[26] M. Fadel, M.F. Riley and J.F.M. Barthelemy, Two-point exponential approximation method for structural optimization, *Structural Optimization*, **2**, 1990, 117–124.